Supporting Information Material for

Computational Evaluation of the Oxidation of Superoxide to Molecular Dioxygen Mediated by NNNN-Tetradentate Copper Complexes

Table S1. Complexes and corresponding IUPAC names.

Complex	IUPAC name
1	(1E,1'E)-N,N'-(ethane-1,2-diyl)bis(1-(pyridin-2-yl)methanimine)copper(II)
2	(1E,1'E)-N,N'-(propane-1,3-diyl)bis(1-(pyridin-2-yl)methanimine)copper(II)
3	(1E,1'E)-N,N'-(1,2-phenylene)bis(1-(pyridin-2-yl)methanimine)copper(II)
4	(1E,1'E)-N,N'-(4,5-dimethyl-1,2-phenylene)bis(1-(pyridin-2-yl)methanimine)copper(II)
5	(1E,1'E)-N,N'-(3,5-dimethyl-1,2-phenylene)bis(1-(pyridin-2-yl)methanimine)copper(II)
6	(1E,1'E)-N,N'-(4,5-dichloro-1,2-phenylene)bis(1-(pyridin-2-yl)methanimine)copper(II)
7	(1E,1'E)-N,N'-(naphthalene-1,8-diyl)bis(1-(pyridin-2-yl)methanimine)copper(II)
8	(1E,1'E)-N,N'-(1,2-diphenylethane-1,2-diyl)bis(1-(pyridin-2-yl)methanimine)copper(II)
9	(1E,1'E)-N,N'-(4-benzyl-1,2-phenylene)bis(1-(pyridin-2-yl)methanimine)copper(II)

The Gibbs reaction energies were determined using the thermodynamic data obtained from optimization and frequency calculations. This enables the calculation of the Gibbs energies for both the products and reactants of the reaction under study. The difference between these two energies yields the reaction energy. The following equation summarizes this procedure:

$$\Delta_r G° = \sum (EE_0 + C_{Gibbs})_{products} - \sum (EE_0 + C_{Gibbs})_{reactants}$$

Where $\Delta_r G°$ represents the Gibbs reaction energy change on standard conditions, EE_0 is the electronic energy, and C_{Gibbs} is a correction term to the Gibbs energy due to temperature. The thermodynamic values used in the calculations are shown in table S2, where the C_H is a correction term to the enthalpy energy due to temperature.

Table S2. Thermodynamic values of the molecules involved in the considered reactions given in hartrees. E_0 is the electronic energy, C_{Gibbs} and C_{H} are the thermal correction to free energy and enthalpy at 298.15 K, respectively.

Molecules	E_0	C_{Gibbs}	C_H
O_2	-150.308589	-0.015912	0.007332
H_2O	-76.420906	0.003990	0.025404
H_2O_2	-151.533993	0.005045	0.030314
$O_2^{\cdot-}$	-150.322373	-0.016844	0.006230
Complex-1-Cu(II)	-2401.004539	0.220809	0.281963
Complex-1-Cu(I)	-2401.149408	0.217053	0.280797
Complex-1-Cu(II)-superoxide	-2551.469617	-0.034591	0.011641
Complex-1-Cu(I)-dioxygen	-2551.463981	-0.034925	0.012587
Complex-1-Cu(II)(OH^-)	-2477.143734	0.220432	0.280322
Complex-1-Cu(I)(H_2O)	-2477.587722	0.233556	0.307676
Complex-1-Cu(I)(H^+)	-2401.593503	0.232577	0.295536
Complex-2-Cu(II)	-2440.311348	0.250296	0.312963
Complex-2-Cu(I)	-2440.452901	0.241776	0.310711
Complex-2-Cu(II)-superoxide	-2590.776515	-0.034657	0.011669
Complex-2-Cu(I)-dioxygen	-2590.766547	-0.036233	0.012558
Complex-2-Cu(II)(OH^-)	-2471.839025	0.257954	0.327592
Complex-2-Cu(I)(H_2O)	-2472.310666	0.271377	0.341222

Complex-2-Cu(I)(H^+)	-2440.903328	0.259517	0.325563
Complex-3-Cu(II)	-2553.415703	0.243222	0.308536
Complex-3-Cu(I)	-2553.560790	0.237590	0.306004
Complex-3-Cu(II)-superoxide	-2703.857379	-0.033201	0.011895
Complex-3-Cu(I)-dioxygen	-2703.875439	0.236117	0.313900
Complex-3-Cu(II)(OH^-)	-2629,034243	0.251784	0.323311
Complex-3-Cu(I)(H_2O)	-2630.002908	0.257456	0.333686
Complex-3-Cu(I)(H^+)	-2553.994912	0.253644	0.321037
Complex-4-Cu(II)	-2632.031704	0.295305	0.367146
Complex-4-Cu(I)	-2632.175395	0.288801	0.364575
Complex-4-Cu(II)-superoxide	-2782.497630	-0.035027	0.011673
Complex-4-Cu(I)-dioxygen	-2782.489934	-0.037379	0.012564
Complex-4-Cu(II)(OH^-)	-2708.152507	0.303918	0.382215
Complex-4-Cu(I)(H_2O)	-2708.617184	0.308799	0.392061
Complex-4-Cu(I)(H^+)	-2632.610851	0.305571	0.379758
Complex-5-Cu(II)	-2632.026911	0.295013	0.367196
Complex-5-Cu(I)	-2632.172088	0.289055	0.365025
Complex-5-Cu(II)-superoxide	-2782.492720	-0.035916	0.011641
Complex-5-Cu(I)-dioxygen	-2782.486574	-0.035998	0.011591
Complex-5-Cu(II)(OH^-)	-2708.188273	0.303954	0.382174
Complex-5-Cu(I)(H_2O)	-2708.614012	0.308523	0.392217
Complex-5-Cu(I)(H^+)	-2632.606911	0.304974	0.379781
Complex-6-Cu(II)	-3472.607672	0.219869	0.291739
Complex-6-Cu(I)	-3472.755761	0.213893	0.289163
Complex-6-Cu(II)-superoxide	-3623.051466	-0.038512	0.012559
Complex-6-Cu(I)-dioxygen	-3623.070309	-0.037466	0.012567
Complex-6-Cu(II)(OH^-)	-3548.73387	0.233027	0.314254

Complex-6-Cu(I)(H_2O)	-3549.197586	0.233495	0.316723
Complex-6-Cu(I)(H^+)	-3473.186255	0.230125	0.304122
Complex-7-Cu(II)	-2707.030448	0.288865	0.358533
Complex-7-Cu(I)	-2707.175073	0.282068	0.356475
Complex-7-Cu(II)-superoxide	-2857.494712	-0.036243	0.011657
Complex-7-Cu(I)-dioxygen	-2857.489731	-0.036904	0.012575
Complex-7-Cu(II)(OH^-)	-2783.153883	0.301652	0.379312
Complex-7-Cu(I)(H_2O)	-2783.614806	0.302571	0.383721
Complex-7-Cu(I)(H^+)	-2707.602564	0.295491	0.370163
Complex-8-Cu(II)	-2863.035325	0.372637	0.454142
Complex-8-Cu(I)	-2863.180329	0.366381	0.452062
Complex-8-Cu(II)-superoxide	-3013.500868	-0.036663	0.011642
Complex-8-Cu(I)-dioxygen	-3013.494944	-0.038029	0.012559
Complex-8-Cu(II)(OH^-)	-2888.191773	0.302721	0.408612
Complex-8-Cu(I)(H_2O)	-2888.700970	0.351914	0.420254
Complex-8-Cu(I)(H^+)	-2863.611753	0.380402	0.466259
Complex-9-Cu(II)	-2823.736699	0.342557	0.423741
Complex-9Cu(I)	-2823.882307	0.337517	0.421862
Complex-9-Cu(II)-superoxide	-2974.202979	-0.035804	0.011677
Complex-9-Cu(I)-dioxygen	-2974.197266	-0.036739	0.012601
Complex-9-Cu(II)(OH^-)	-2899.832723	0.328235	0.414284
Complex-9-Cu(I)(H_2O)	-2900.323729	0.355506	0.449066
Complex-9-Cu(I)(H^+)	-2824.316322	0.352596	0.436663

The H^+ free energy employed in mechanisms 1 and 2 was computed as the addition of its experimental Gibbs free energy of formation and the corresponding solvation energy, being equal to −0.4337 Hartree..[1,2]

1. A. Malloum, J. J. Fifen and J. Conradie, *J. Mol. Liq.*, 2021, **322**, 114919.

2. M. D. Tissandier, K. A. Cowen, W. Y. Feng, E. Gundlach, M. H. Cohen, A. D. Earhart, J. V. Coe and T. R. Tuttle, *J. Phys. Chem. A*, 1998, **102**, 7787–7794.

Table S3. Changes in the Gibbs energy of reaction for the three considered mechanisms.

	Δ*G* (kcal/mol)					
	Mechanism 1		**Mechanism 2**		**Mechanism 3**	
Complexes	**Step 1**	**Step 2**	**Step 1**	**Step 2**	**Step 1**	**Step 2**
1	–2.0	–462.4	–80.8	–94.0	–79.4	–104.6
2	–6.1	–168.6	–84.3	–90.5	–77.5	–106.4
3	–6.9	–167.9	–75.5	–99.2	–81.0	–98.64
4	–7.1	–167.6	–75.6	–99.2	–80.4	–98.97
5	–7.3	–167.4	–76.3	–98.4	–82.1	–89.14
6	–9.3	–165.5	–75.2	–99.5	–82.9	–87.30
7	–7.2	–167.5	–73.4	–101.3	–81.5	–88.96
8	–7.2	–167.5	–75.4	–99.3	–81.2	–89.06
9	–9.6	–165.2	–76.0	–98.7	–80.8	–278.5

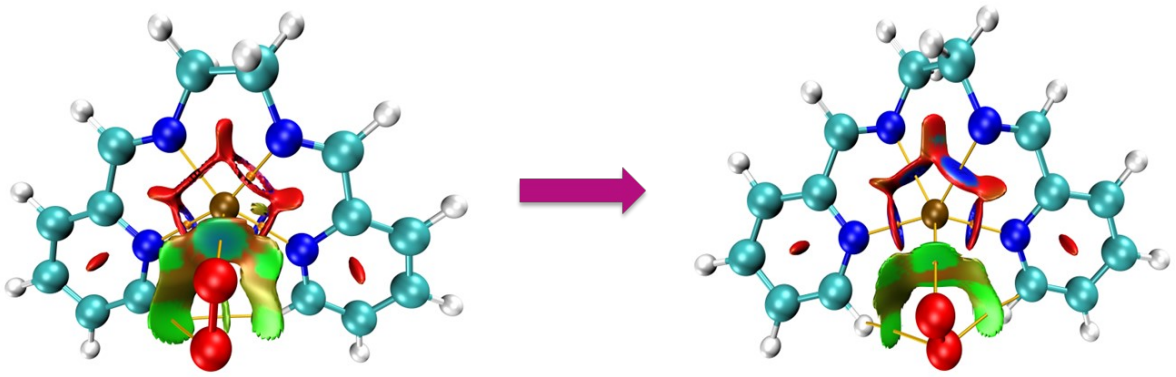

Figure S1. Left, NCI graph of the Complex **1** (ox) with the superoxide radical. Right, NCI graph of the Complex **1** (red) with the oxygen.

Table S4. Atomic charges and spin densities for the copper cation and oxygens involved in the dismutation reaction for complexes **1**.

Complex 1 - superoxide		
Atom	**Atomic charge**	**Spin density**
Cu(II)	1.3993	0.8257
O	– 0.4720	0.5178
O	– 0.4887	0.4685
Complex 1 - dioxygen		
Atom	**Atomic charge**	**Spin density**
Cu(I)	0.6128	0.0051
O	– 0.0072	0.9950
O	– 0.0118	0.9953

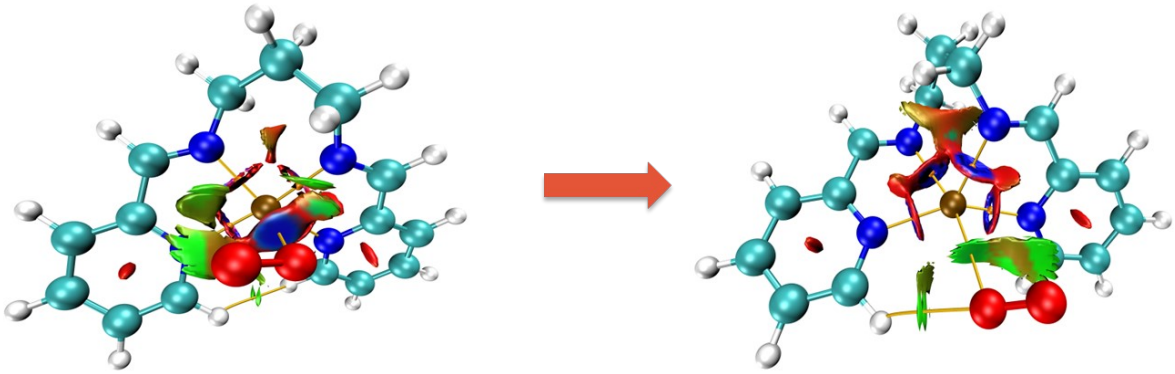

Figure S2. Left, NCI graph of the Complex **2** (ox) with the superoxide radical. Right, NCI graph of the Complex **2** (red) with the oxygen.

Table S5. Atomic charges and spin densities for the copper cation and oxygens involved in the dismutation reaction for complexes **2**.

Complex 2 - superoxide		
Atom	**Electronic charge**	**Spin density**
Cu	1.4258	0.8225
O	– 0.4597	0.4826
O	– 0.4707	0.5203
Complex 2 - dioxygen		
Atom	**Electronic density**	**Spin density**
Cu	1.0145	0.0097
O	– 0.0162	0.9924
O	– 0.0089	0.9937

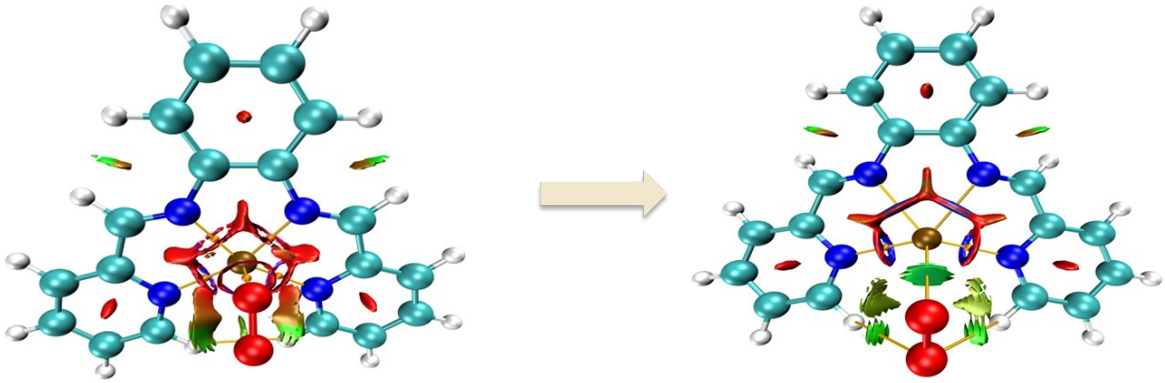

Figure S3. Left, NCI graph of the Complex **3** with the superoxide radical. Right, NCI graph of the Complex **3** complex with oxygen.

Table S6. Atomic charges and spin densities for the copper cation and oxygens involved in the dismutation reaction for complexes **3**.

Complex 3 - superoxide		
Atom	**Electronic charge**	**Spin density**
Cu	1.6599	0.8553
O	– 0.4330	0.5821
O	– 0.3730	0.5360
Complex 3 - dioxygen		
Atom	**Electronic charge**	**Spin density**
Cu	0.6128	0.0051
O	– 0.0072	0.9950
O	– 0.0118	0.9952

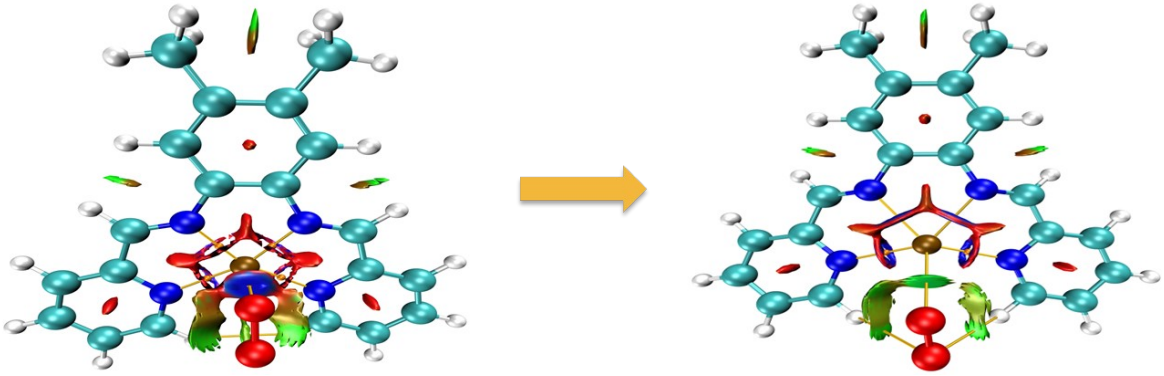

Figure S4. Left, NCI graph of the Complex **4** with the superoxide radical. Right, NCI graph of the Complex **4** complex with oxygen.

Table S7. Atomic charges and spin densities for the copper cation and oxygens involved in the dismutation reaction for complexes **4**.

Complex 4 - superoxide		
Atom	**Atomic charge**	**Spin density**
Cu(II)	1.5226	0.8271
O	– 0.4708	0.5243
O	– 0.4586	0.4763
Complex 4 - dioxygen		
Atom	**Atomic charge**	**Spin density**
Cu(I)	1.1267	0.0106
O	– 0.0061	0.9931
O	– 0.0094	0.9896

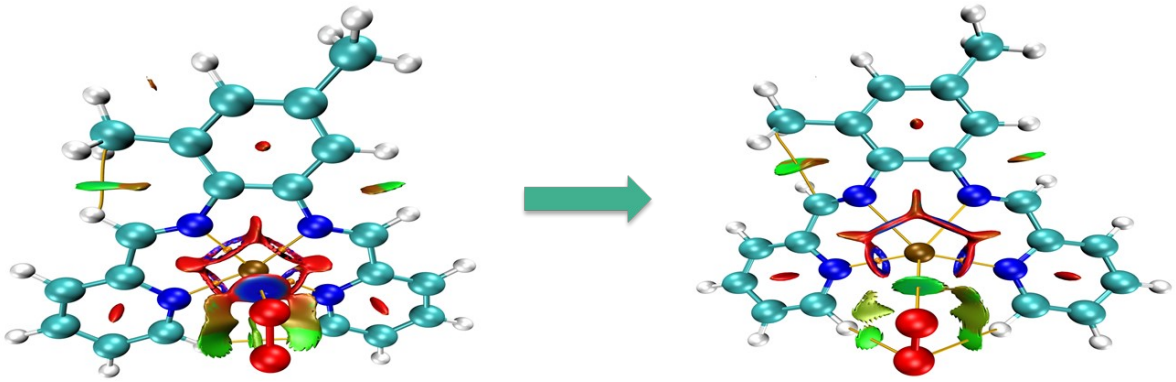

Figure S5. Left, NCI graph of the Complex **5** complex with the superoxide radical. Right, NCI graph of the Complex **5** complex with the oxygen.

Table S8. Atomic charges and spin densities for the copper cation and oxygens involved in the dismutation reaction for complexes **5**.

Complex 5 - superoxide		
Atom	**Electronic charge**	**Spin density**
Cu	1.3271	0.8260
O	– 0.4708	0.5246
O	– 0.4675	0.4765
Complex 5 – dioxygen		
Atom	**Electronic charge**	**Spin density**
Cu	0.4749	0.0116
O	– 0.0084	0.9933
O	– 0.0198	0.9879

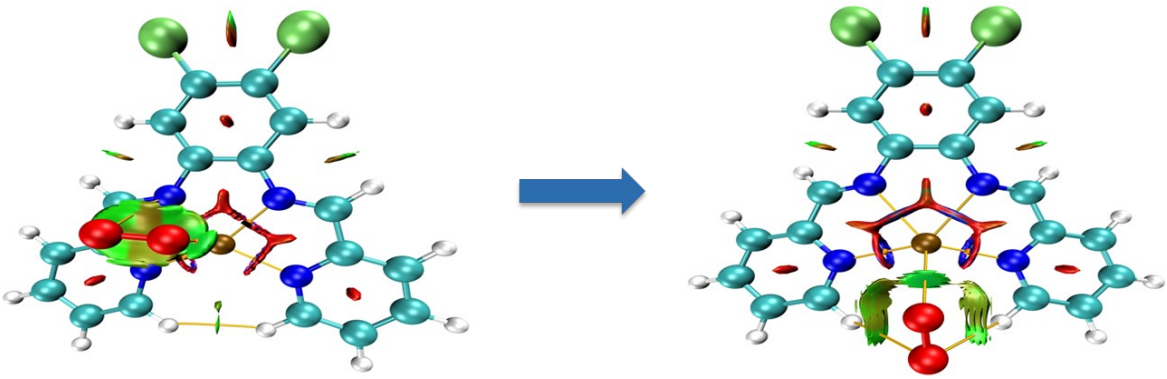

Figure S6. Left, NCI graph of the Complex **6** with the superoxide radical. Right, NCI graph of the Complex **6** with oxygen.

Table S9. Atomic charges and spin densities for the copper cation and oxygens involved in the dismutation reaction for complexes **6**.

Complex 6 - superoxide		
Atom	**Electronic charge**	**Spin density**
Cu	1.6680	0.8314
O	– 0.4441	0.4708
O	– 0.4758	0.5310
Complex 6 - dioxygen		
Atom	**Electronic charge**	**Spin density**
Cu	1.1051	0.0104
O	– 0.0103	0.9939
O	– 0.0067	0.9895

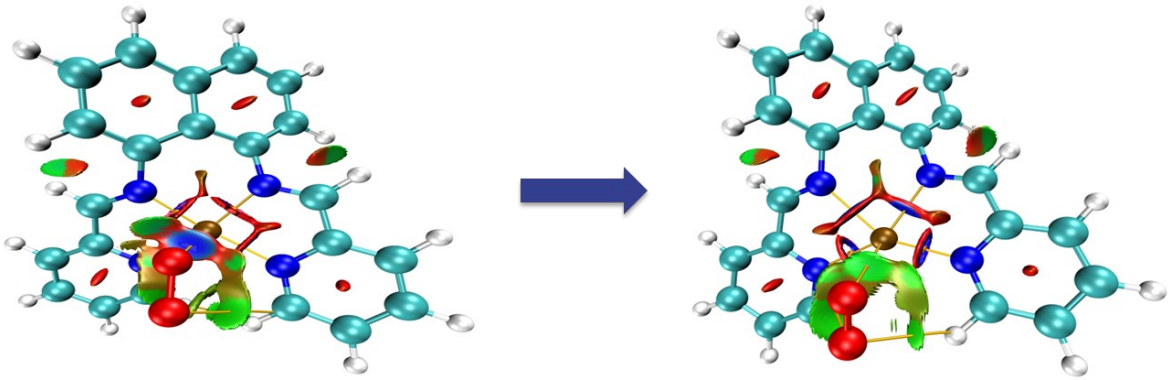

Figure S7. Left, NCI graph of the Complex **7** with the superoxide radical. Right, NCI graph of the Complex **7** with oxygen.

Table S10. Atomic charges and spin densities for the copper cation and oxygens involved in the dismutation reaction for complexes **7**.

Complex 7 - superoxide		
Atom	**Electronic charge**	**Spin density**
Cu	1.6132	0.8283
O	– 0.4703	0.5178
O	– 0.4657	0.4847
Complex 7 – dioxygen		
Atom	**Electronic charge**	**Spin density**
Cu	1.0985	0.0063
O	– 0.0065	0.9928
O	– 0.0108	0.9945

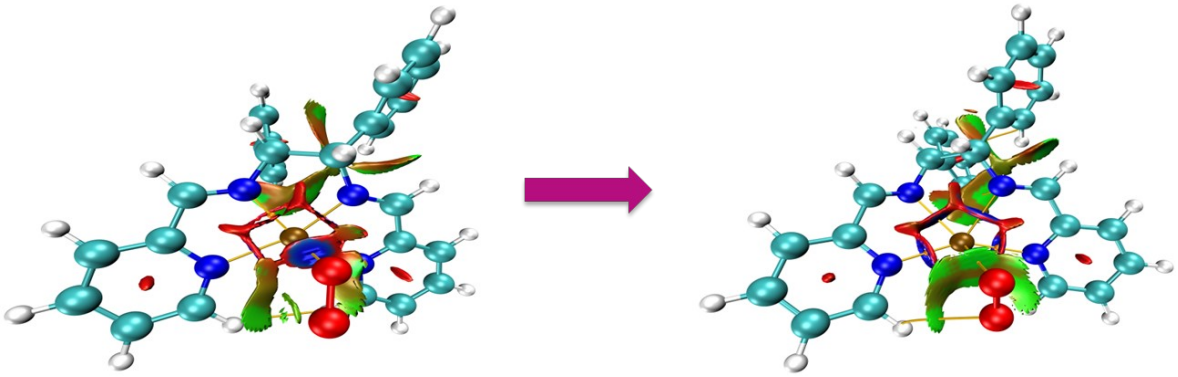

Figure S8. Left, NCI graph of the Complex **8** with the superoxide radical. Right, NCI graph of the Complex **8** with oxygen.

Table S11. Atomic charges and spin densities for the copper cation and oxygens involved in the dismutation reaction for complexes **8**.

Complex 8 - superoxide		
Atom	**Electronic charge**	**Spin density**
Cu	1.6222	0.8355
O	– 0.4981	0.4375
O	– 0.4454	0.5415
Complex 8 – dioxygen		
Atom	**Electronic charge**	**Spin density**
Cu	0.1229	0.0042
O	– 0.0064	0.9952
O	– 0.0098	0.9959

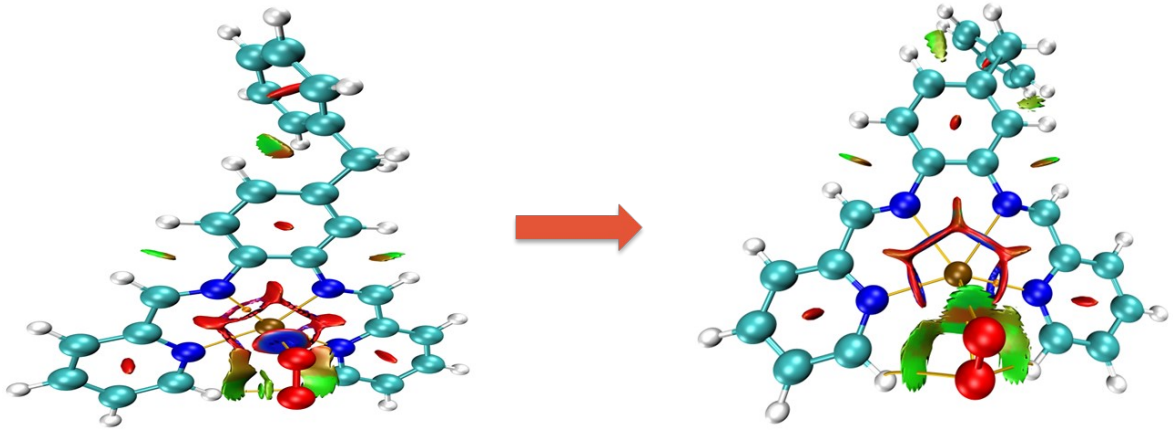

Figure S9. Left, NCI graph of the Complex **9** with the superoxide radical. Right, NCI graph of the Cu(I)-11C4 Complex **9** with oxygen.

Table S12. Atomic charges and spin densities for the copper cation and oxygens involved in the dismutation reaction for complexes **9**.

Complex 9 - superoxide		
Atom	**Electronic charge**	**Spin density**
Cu	1.3946	0.8269
O	– 0.4738	0.5261
O	– 0.4543	0.4747
Complex 9 - dioxygen		
Atom	**Electronic charge**	**Spin density**
Cu	– 0.7828	0.0065
O	– 0.0030	0.9951
O	– 0.0088	0.9950

Table S13. Topological parameters calculated for the complex **1** from the electronic density distribution at the BCP.

BCP	$\rho(r)$	$\nabla^2\rho(r)$	V(r)	G(r)	|V(r)| / G(r)	H	Elipticity
1(ox) + $O_2^{\bullet -}$							
1	0.0790	0.3648	-0.1148	0.1030	1.11	-0.0117	0.0172
2	0.0790	0.3649	-0.1147	0.1030	1.11	-0.0117	0.0192
3	0.0675	0.2936	-0.0920	0.0827	1.11	-0.0093	0.0764
4	0.0675	0.2939	-0.0921	0.0828	1.11	-0.0093	0.0761
5	0.0201	0.0764	-0.0217	0.0204	1.06	-0.0013	0.1925
1(red) + O_2							
1	0.0385	0.1372	-0.0484	0.0414	1.17	-0.0071	0.0469
2	0.0385	0.1371	-0.0484	0.0413	1.17	-0.0071	0.0487
3	0.0608	0.2722	-0.0879	0.0780	1.13	-0.0099	0.0455
4	0.0608	0.2723	-0.0880	0.0780	1.13	-0.0099	0.0443
5	0.0102	0.0419	-0.0087	0.0096	0.91	0.0009	0.4038

Table S14. Topological parameters calculated for the complex **2** from the electronic density distribution at the BCP.

BCP	$\rho(r)$	$\nabla^2\rho(r)$	V(r)	G(r)	|V(r)| / G(r)	H	Elipticity
2(ox) + $O_2^{\bullet -}$							
1	0.0764	0.3542	-0.1105	0.0995	1.1106	-0.0110	0.0441
2	0.0762	0.3533	-0.1099	0.0991	1.1090	-0.0108	0.0589
3	0.0685	0.3068	-0.0950	0.0859	1.1059	-0.0091	0.0452
4	0.0688	0.3081	-0.0960	0.0865	1.1098	-0.0095	0.0403
5	0.0362	0.1385	-0.0449	0.0398	1.1281	-0.0051	0.0897
2(red) + O_2							
1	0.0486	0.1902	-0.0654	0.0565	1.1575	-0.0089	0.0512

2	0.0485	0.1903	-0.0654	0.0565	1.1575	-0.0089	0.0521
3	0.0590	0.2605	-0.0848	0.0749	1.1322	-0.0099	0.0694
4	0.0590	0.2612	-0.0850	0.0751	1.1318	-0.0099	0.0680
5	0.0111	0.0417	-0.0089	0.0097	0.9175	0.0008	0.1294

Table S15. Topological parameters calculated for the complex **3** from the electronic density distribution at the BCP.

BCP	$\rho(r)$	$\nabla^2\rho(r)$	V(r)	G(r)	|V(r)| / G(r)	H	Elipticity
3(ox) + $O_2^{\bullet -}$							
1	0.0768	0.3649	-0.1163	0.1037	1.1215	-0.0126	0.0937
2	0.0769	0.3660	-0.1167	0.1041	1.1210	-0.0126	0.0898
3	0.0704	0.3240	-0.1023	0.0916	1.1168	-0.0107	0.0799
4	0.0703	0.3236	-0.1018	0.0914	1.1138	-0.0104	0.0843
5	0.0746	0.4047	-0.1085	0.1048	1.0353	-0.0037	0.0914
3(red) + O_2							
1	0.0379	0.1355	-0.0477	0.0408	1.1691	-0.0069	0.0424
2	0.0378	0.1354	-0.0476	0.0407	1.1695	-0.0069	0.0424
3	0.0588	0.2599	-0.0843	0.0746	1.1300	-0.0097	0.0327
4	0.0588	0.2600	-0.0844	0.0747	1.1299	-0.0097	0.0328
5	0.0144	0.0572	-0.0138	0.0140	0.9857	0.0002	0.0935

Table S16. Topological parameters calculated for the complex **4** from the electronic density distribution at the BCP.

BCP	$\rho(r)$	$\nabla^2\rho(r)$	V(r)	G(r)	|V(r)| / G(r)	H	Elipticity
4(ox) + $O_2^{\bullet -}$							
1	0.0756	0.3515	-0.1095	0.0987	1.1094	-0.0108	0.0059
2	0.0755	0.3514	-0.1094	0.0986	1.1095	-0.0108	0.0072

3	0.0697	0.3091	-0.0966	0.0869	1.1116	-0.0097	0.0782
4	0.0697	0.3090	-0.0967	0.0870	1.1115	-0.0097	0.0772
5	0.0384	0.1513	-0.0485	0.0432	1.1227	-0.0053	0.1028
4(red) + O_2							
1	0.0397	0.1443	-0.0507	0.0434	1.1682	-0.0073	0.0456
2	0.0397	0.1443	-0.0507	0.0434	1.1682	-0.0073	0.0457
3	0.0575	0.2520	-0.0821	0.0725	1.1324	-0.0096	0.0311
4	0.0575	0.2519	-0.0820	0.0725	1.1310	-0.0095	0.0310
5	0.0127	0.0506	-0.0115	0.0121	0.9504	0.0006	0.1159

Table S17. Topological parameters calculated for the complex **5** from the electronic density distribution at the BCP.

BCP	$\rho(r)$	$\nabla^2\rho(r)$	V(r)	G(r)	|V(r)| / G(r)	H	Elipticity
5(ox) + $O_2^{\bullet -}$							
1	0.0725	0.3301	-0.1031	0.0928	1.1110	-0.0103	0.0092
2	0.0786	0.3720	-0.1160	0.1044	1.1111	-0.0116	0.0062
3	0.0725	0.3280	-0.1024	0.0922	1.1106	-0.0102	0.0730
4	0.0682	0.2997	-0.0939	0.0844	1.1126	-0.0095	0.0666
5	0.0382	0.1501	-0.0483	0.0429	1.1259	-0.0054	0.1034
5(red) + O_2							
1	0.0416	0.1540	-0.0539	0.0462	1.1667	-0.0077	0.0512
2	0.0357	0.1241	-0.0438	0.0374	1.1711	-0.0064	0.0396
3	0.0575	0.2512	-0.0820	0.0724	1.1326	-0.0096	0.0366
4	0.0605	0.2714	-0.0876	0.0777	1.1274	-0.0099	0.0302
5	0.0141	0.0560	-0.0134	0.0137	0.9781	0.0003	0.0968

Table S18. Topological parameters calculated for the complex **6** from the electronic density distribution at the BCP.

BCP	$\rho(r)$	$\nabla^2\rho(r)$	V(r)	G(r)	|V(r)| / G(r)	H	Elipticity
6(ox) + $O_2^{\bullet -}$							
1	0.0746	0.3479	-0.1079	0.0974	1.1073	-0.0105	0.0084
2	0.0745	0.3483	-0.1079	0.0975	1.1065	-0.0104	0.0093
3	0.0699	0.3098	-0.0970	0.0872	1.1121	-0.0098	0.0817
4	0.0700	0.3101	-0.0972	0.0873	1.1125	-0.0098	0.0840
5	0.0415	0.1710	-0.0535	0.0481	1.1114	-0.0054	0.0658
6(red) + O_2							
1	0.0380	0.1367	-0.0480	0.0411	1.1679	-0.0069	0.0428
2	0.0380	0.1367	-0.0480	0.0411	1.1679	-0.0069	0.0428
3	0.0583	0.2573	-0.0835	0.0739	1.1299	-0.0096	0.0331
4	0.0583	0.2573	-0.0835	0.0739	1.1299	-0.0096	0.0331
5	0.0126	0.0508	-0.0115	0.0121	0.9504	0.0006	0.1130

Table S19. Topological parameters calculated for the complex **7** from the electronic density distribution at the BCP.

BCP	$\rho(r)$	$\nabla^2\rho(r)$	V(r)	G(r)	|V(r)| / G(r)	H	Elipticity
7(ox) + $O_2^{\bullet -}$							
1	0.0731	0.3425	-0.1053	0.0954	1.1038	-0.0099	0.0565
2	0.0778	0.3727	-0.1152	0.1042	1.1056	-0.0110	0.0439
3	0.0718	0.3295	-0.1021	0.0922	1.1074	-0.0099	0.0211
4	0.0685	0.3072	-0.0953	0.0861	1.1069	-0.0092	0.0490
5	0.0338	0.1259	-0.0412	0.0363	1.1350	-0.0049	0.1082
7(red) + O_2							
1	0.0422	0.1586	-0.0552	0.0474	1.1646	-0.0078	0.0502

2	0.0402	0.1478	-0.0518	0.0444	1.1667	-0.0074	0.0551
3	0.0649	0.2996	-0.0963	0.0856	1.1250	-0.0107	0.0409
4	0.0657	0.3045	-0.0978	0.0870	1.1241	-0.0108	0.0444
5	0.0103	0.0399	-0.0084	0.0092	0.9130	0.0008	0.1250

Table S20. Topological parameters calculated for the complex **8** from the electronic density distribution at the BCP.

BCP	$\rho(r)$	$\nabla^2\rho(r)$	V(r)	G(r)	|V(r)| / G(r)	H	Elipticity
8(ox) + $O_2^{\bullet -}$							
1	0.0780	0.3616	-0.1136	0.1020	1.1137	-0.0116	0.0197
2	0.0805	0.3763	-0.1187	0.1064	1.1156	-0.0123	0.0174
3	0.0647	0.2769	-0.0871	0.0781	1.1152	-0.0090	0.0738
4	0.0656	0.2832	-0.0888	0.0798	1.1128	-0.0090	0.0713
5	0.0361	0.1542	-0.0466	0.0426	1.0939	-0.0040	0.1481
8(red) + O_2							
1	0.0440	0.1672	-0.0583	0.0500	1.1660	-0.0083	0.0509
2	0.0393	0.1406	-0.0498	0.0425	1.1718	-0.0073	0.0468
3	0.0591	0.2610	-0.0849	0.0751	1.1305	-0.0098	0.0538
4	0.0590	0.2617	-0.0848	0.0751	1.1292	-0.0097	0.0326
5	0.0088	0.0349	-0.0069	0.0078	0.8846	0.0009	0.4142

Table S21. Topological parameters calculated for the complex **9** from the electronic density distribution at the BCP.

BCP	$\rho(r)$	$\nabla^2\rho(r)$	V(r)	G(r)	|V(r)| / G(r)	H	Elipticity
9(ox) + $O_2^{\bullet -}$							
1	0.0767	0.3590	-0.1119	0.1008	1.1101	-0.0111	0.0060
2	0.0758	0.3538	-0.1102	0.0993	1.1098	-0.0109	0.0073

3	0.0691	0.3058	-0.0957	0.0861	1.1115	-0.0096	0.0740
4	0.0697	0.3095	-0.0967	0.0870	1.1115	-0.0097	0.0775
5	0.0394	0.1578	-0.0503	0.0449	1.1203	-0.0054	0.1006
9(red) + O_2							
1	0.0396	0.1447	-0.0508	0.0434	1.1705	-0.0074	0.0444
2	0.0380	0.1359	-0.0479	0.0409	1.1711	-0.0070	0.0408
3	0.0582	0.2562	-0.0833	0.0737	1.1303	-0.0096	0.0302
4	0.0581	0.2564	-0.0833	0.0737	1.1303	-0.0096	0.0273
5	0.0104	0.0453	-0.0096	0.0104	0.9231	0.0008	1.8119

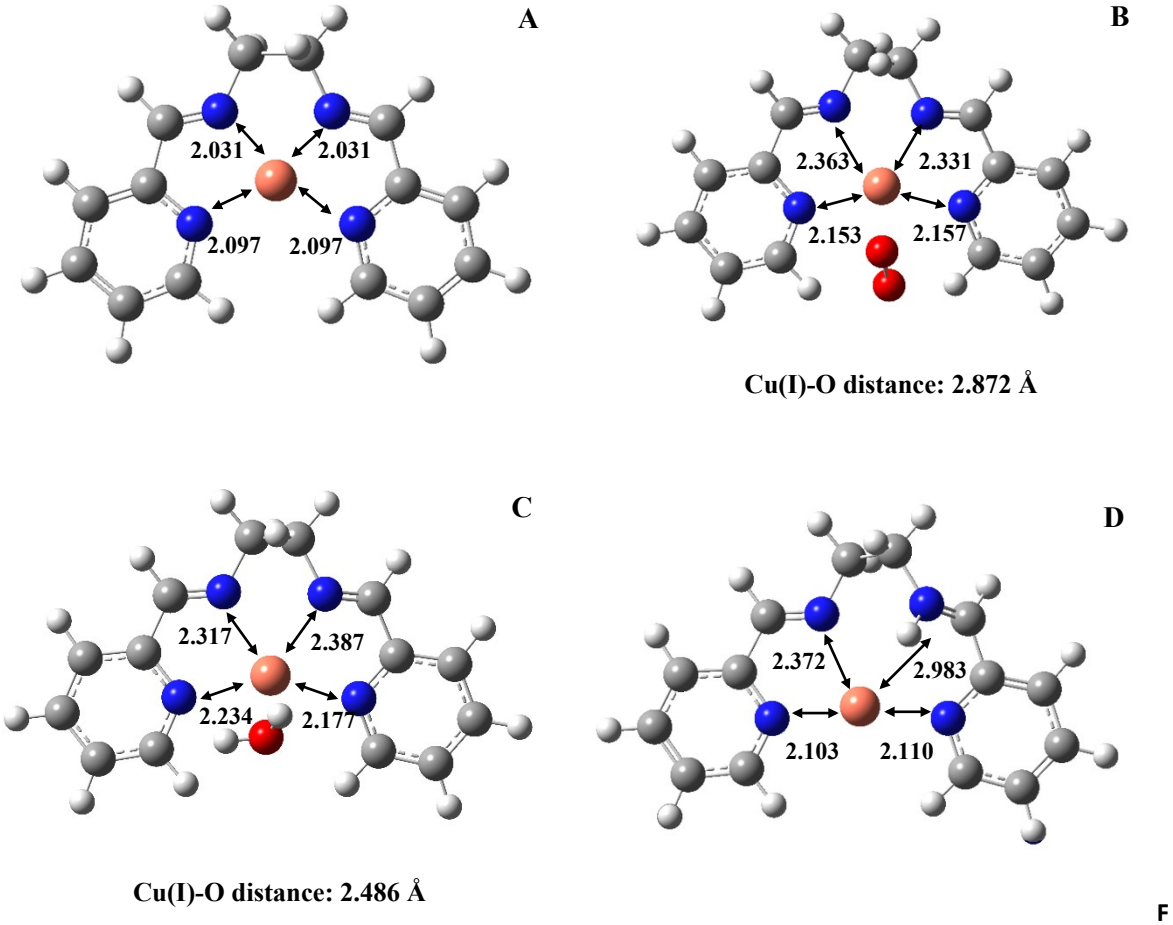

F

igure S11. Optimized structures and distances between copper and nitrogen for: (A) complex 1-Cu(II);(B) reaction intermediate Cu(I)-O_2; (C) reaction intermediate Cu(I)-H_2O; (D) reaction intermediate Cu(I)-H^+. Distances are given in angstroms.

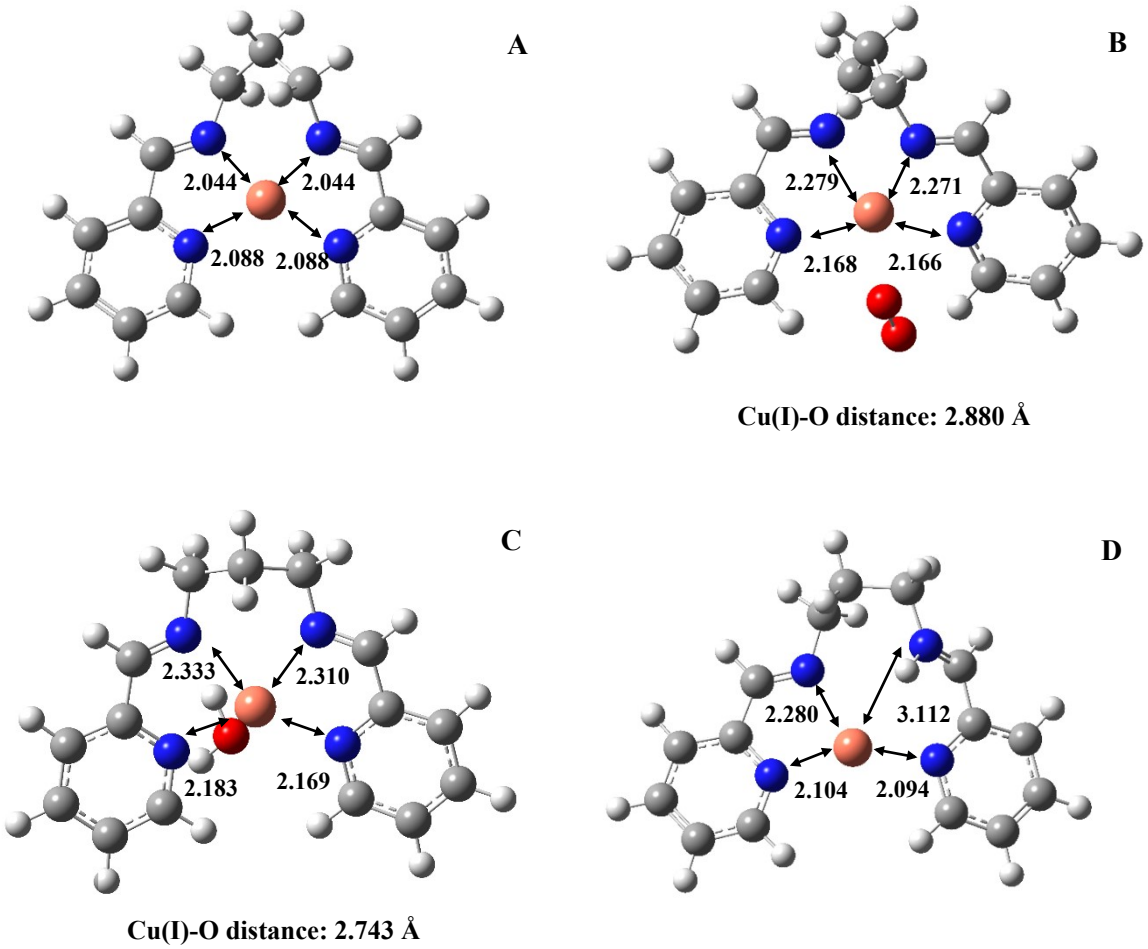

Figure S12. Optimized structures and distances between copper and nitrogen for: (A) complex 2-Cu(II);(B) reaction intermediate Cu(I)-O_2; (C) reaction intermediate Cu(I)-H_2O; (D) reaction intermediate Cu(I)-H^+. Distances are given in angstroms.

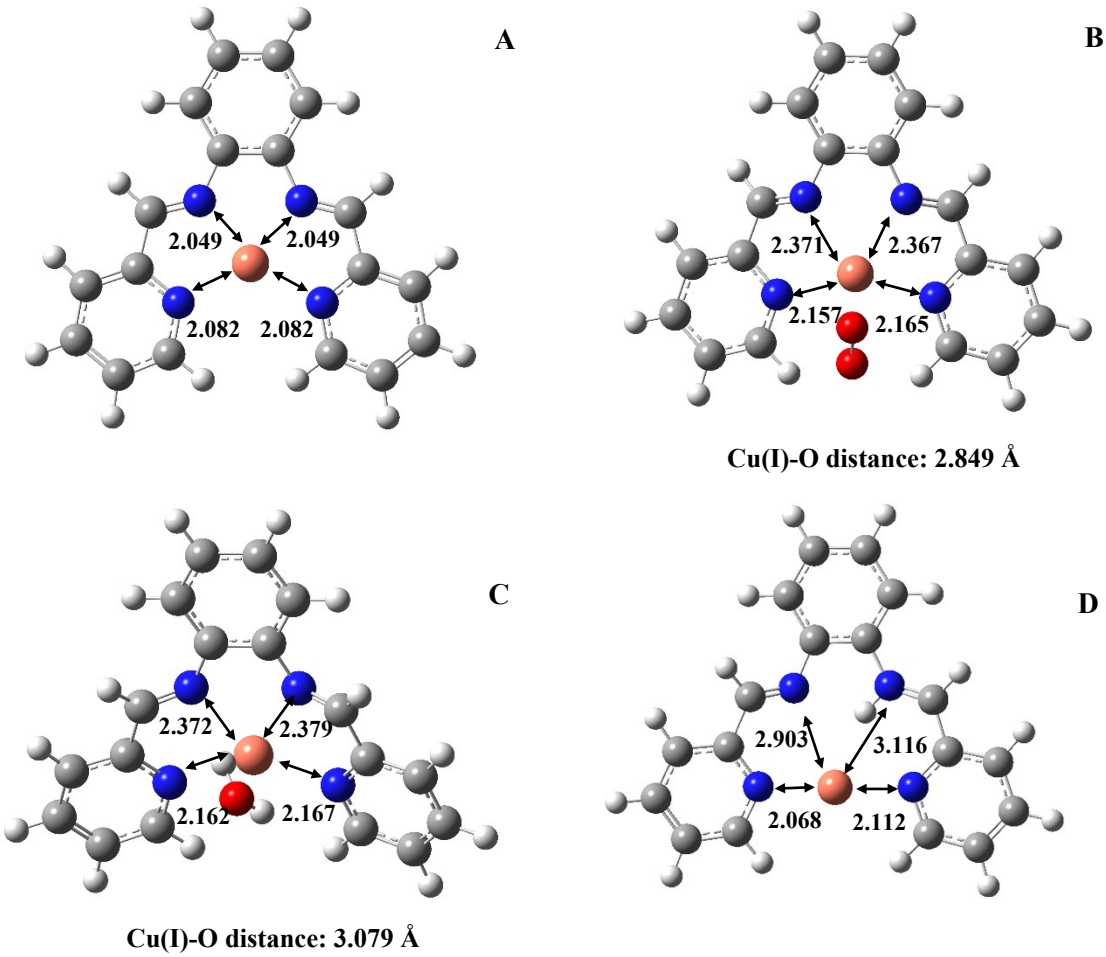

Figure S13. Optimized structures and distances between copper and nitrogen for: (A) complex 3-Cu(II);(B) reaction intermediate Cu(I)-O_2; (C) reaction intermediate Cu(I)-H_2O; (D) reaction intermediate Cu(I)-H^+. Distances are given in angstroms.

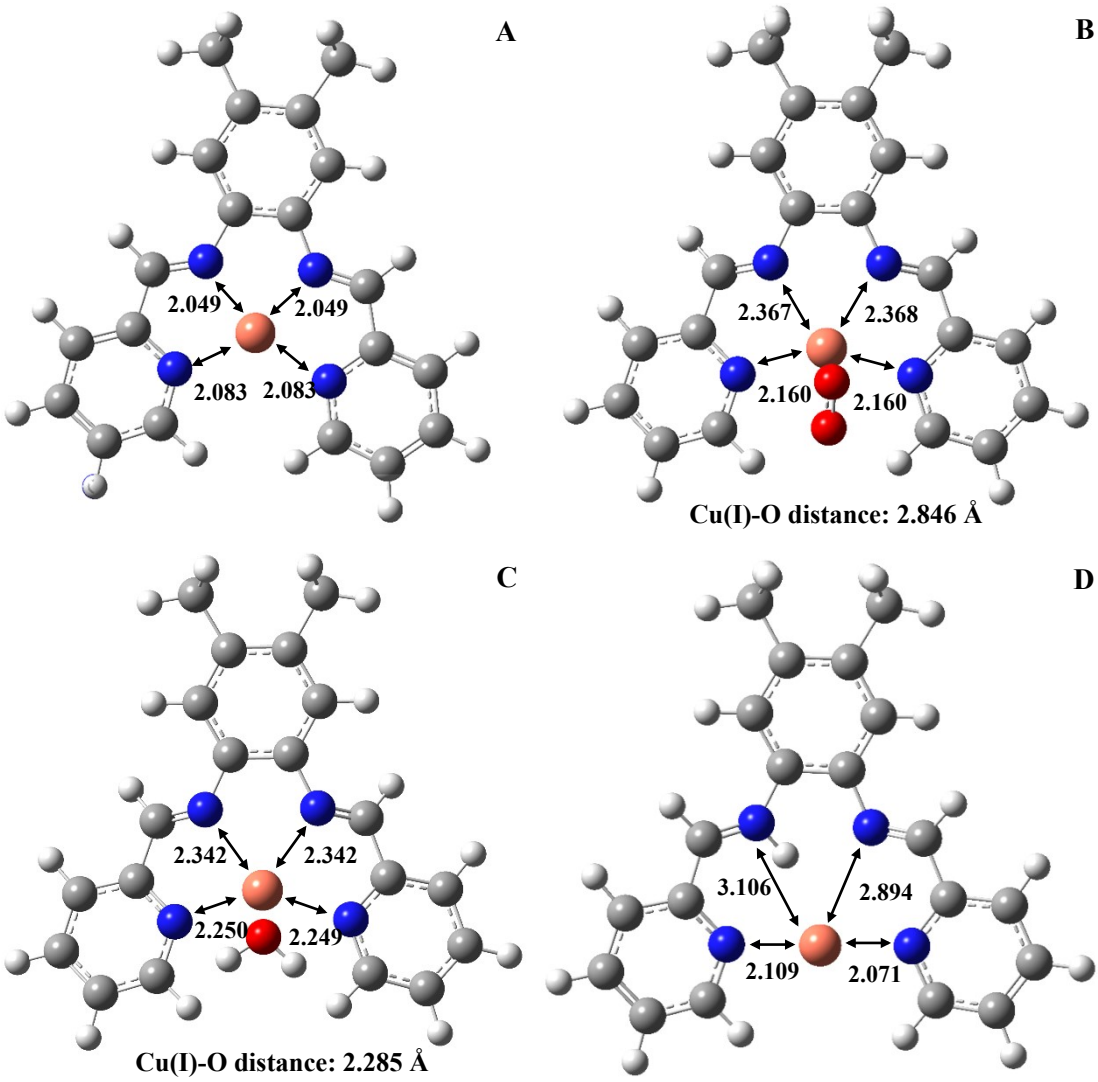

Figure S14. Optimized structures and distances between copper and nitrogen for: (A) complex 4-Cu(II);(B) reaction intermediate Cu(I)-O_2; (C) reaction intermediate Cu(I)-H_2O; (D) reaction intermediate Cu(I)-H^+. Distances are given in angstroms.

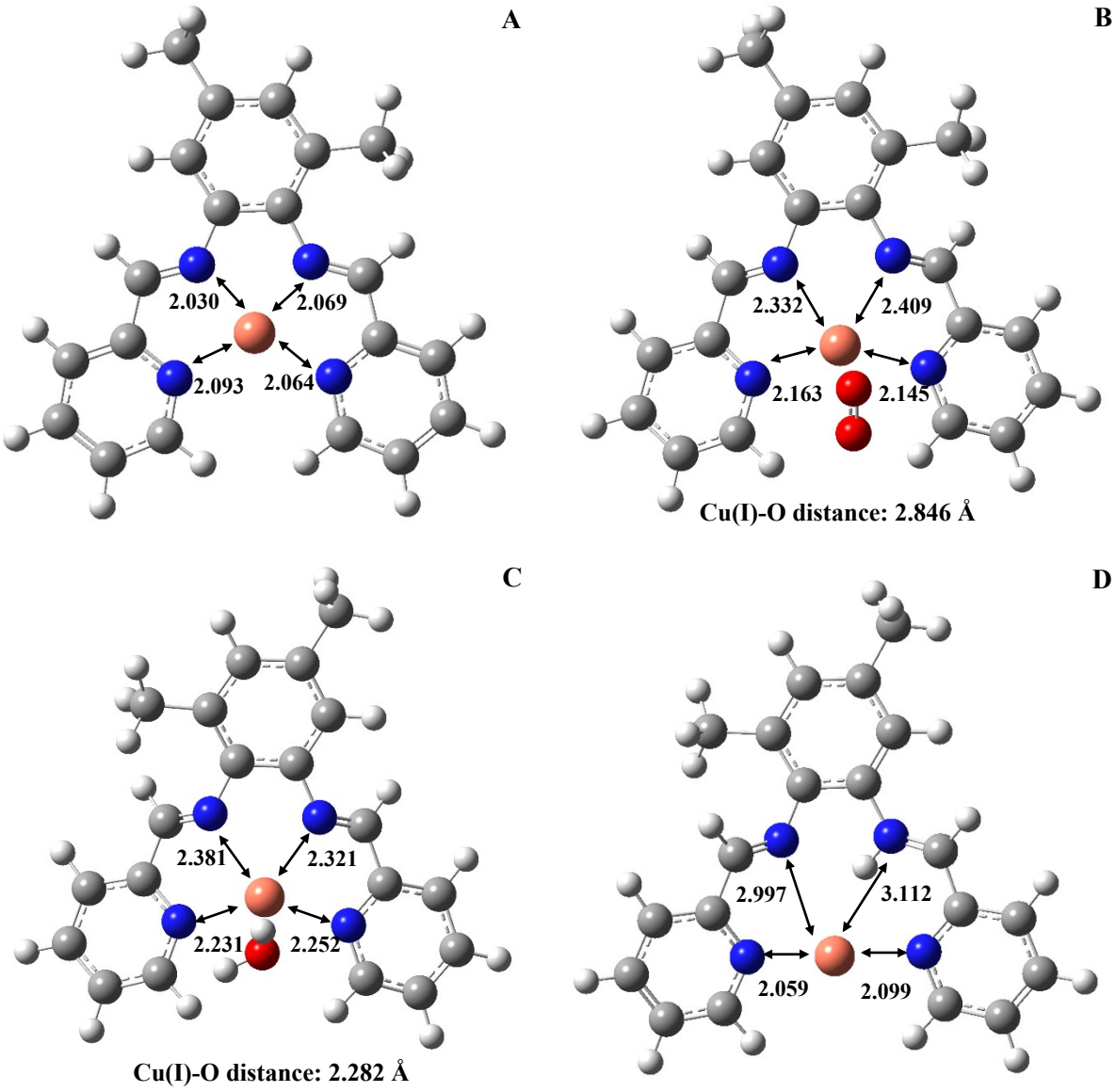

Figure S15. Optimized structures and distances between copper and nitrogen for: (A) complex 5-Cu(II);(B) reaction intermediate Cu(I)-O_2; (C) reaction intermediate Cu(I)-H_2O; (D) reaction intermediate Cu(I)-H^+. Distances are given in angstroms.

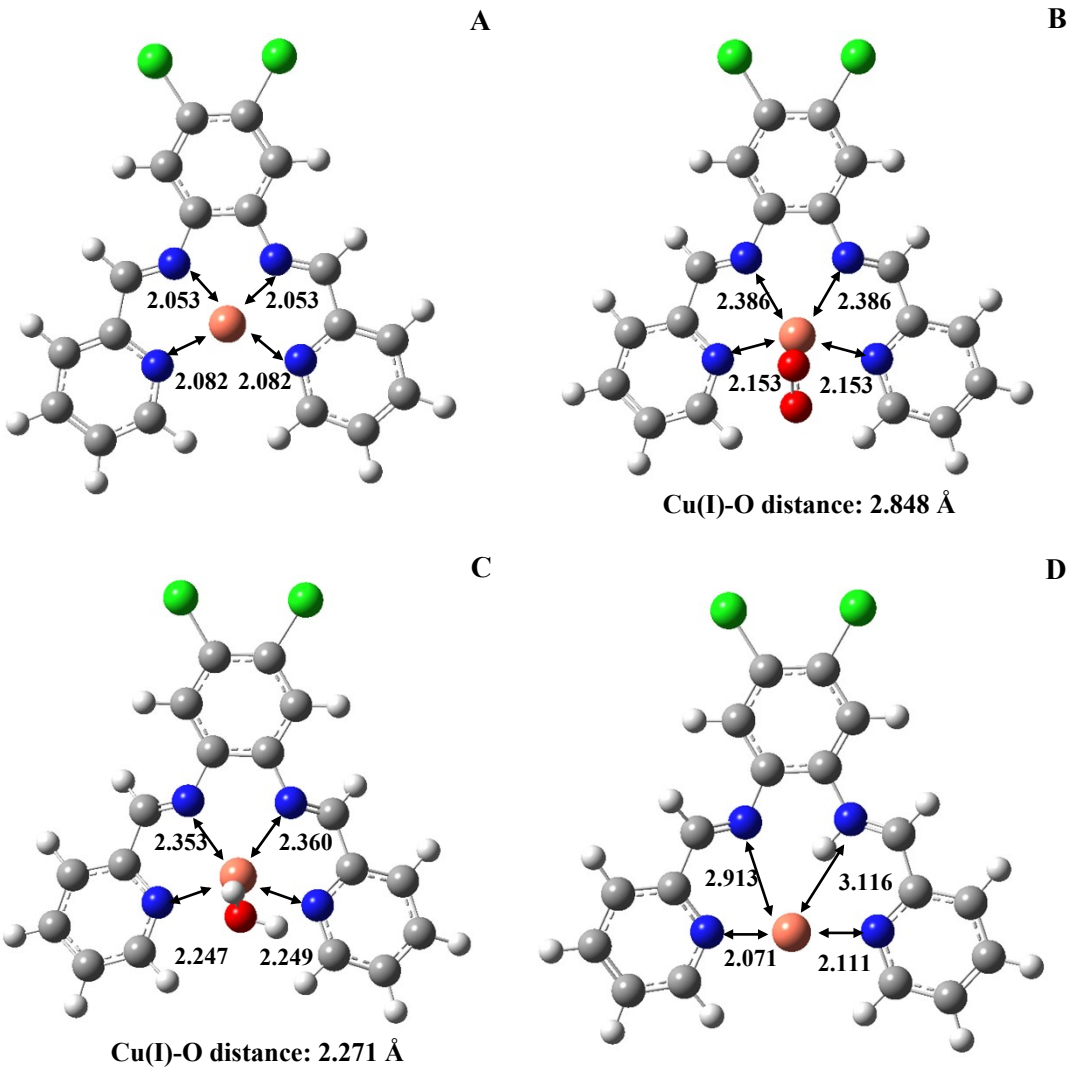

Figure S16. Optimized structures and distances between copper and nitrogen for: (A) complex 6-Cu(II);(B) reaction intermediate Cu(I)-O_2; (C) reaction intermediate Cu(I)-H_2O; (D) reaction intermediate Cu(I)-H^+. Distances are given in angstroms.

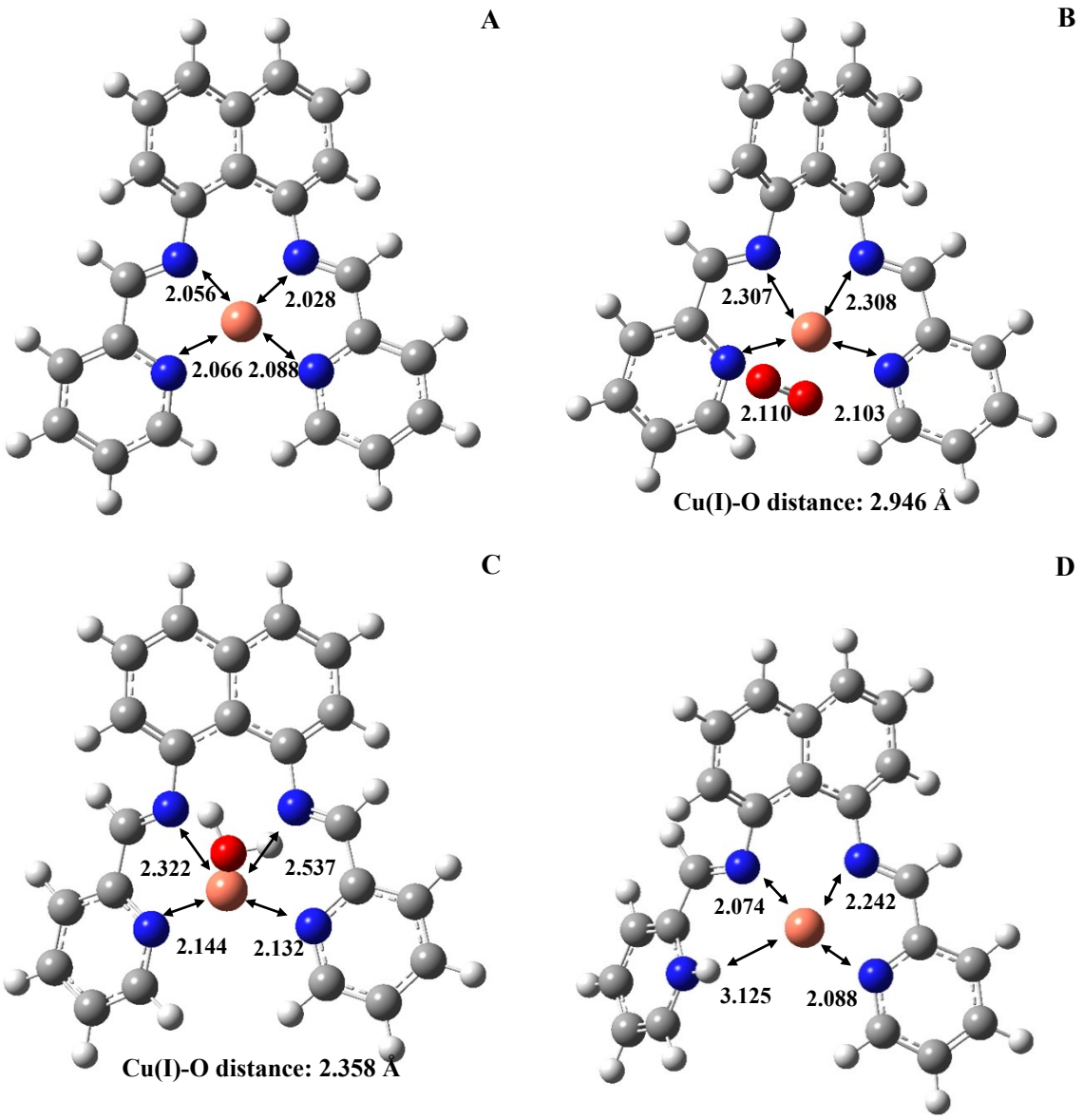

Figure S17. Optimized structures and distances between copper and nitrogen for: (A) complex 7-Cu(II);(B) reaction intermediate Cu(I)-O_2; (C) reaction intermediate Cu(I)-H_2O; (D) reaction intermediate Cu(I)-H^+. Distances are given in angstroms.

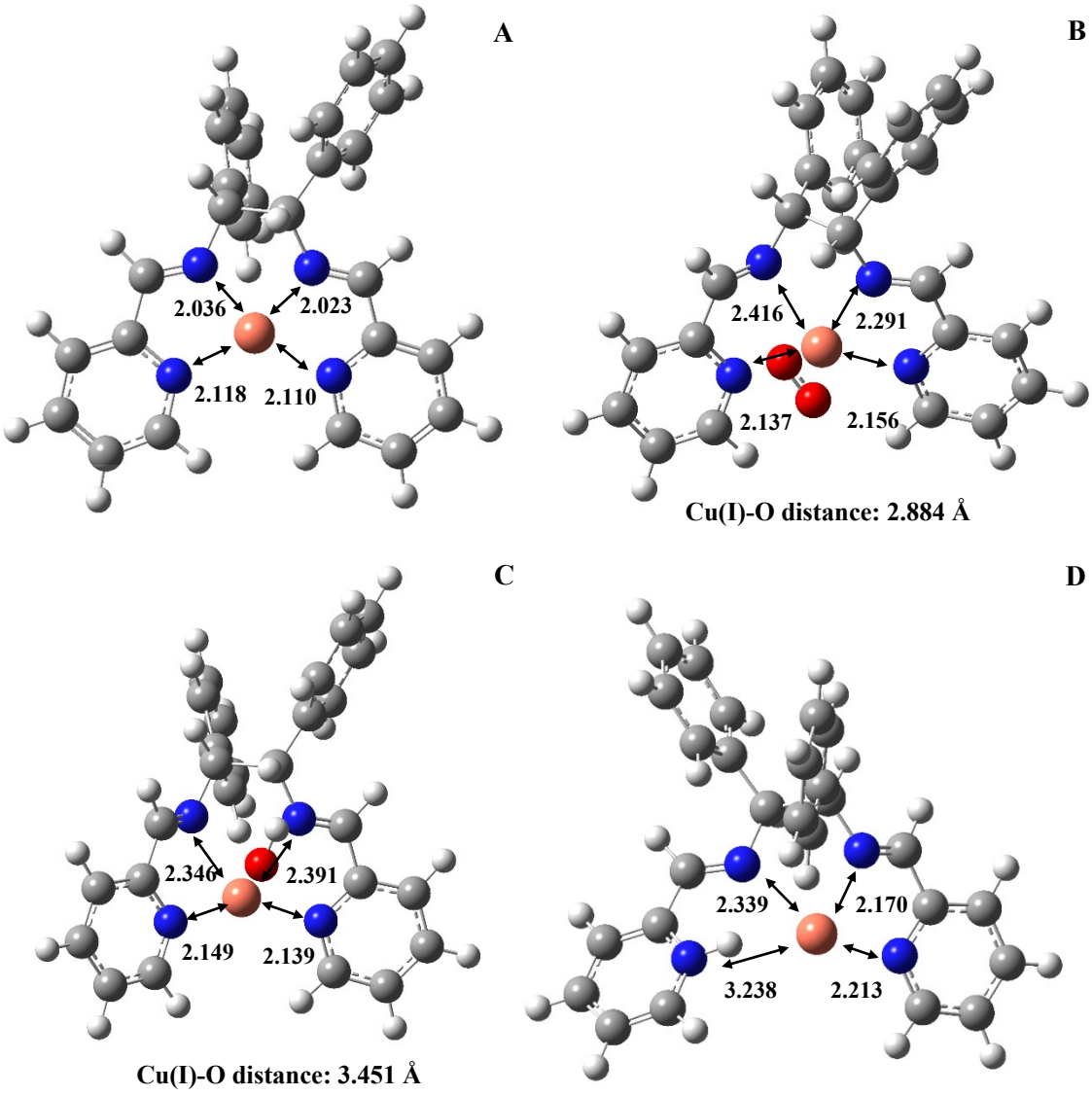

Figure S18. Optimized structures and distances between copper and nitrogen for: (A) complex 8-Cu(II);(B) reaction intermediate Cu(I)-O_2; (C) reaction intermediate Cu(I)-H_2O; (D) reaction intermediate Cu(I)-H^+. Distances are given in angstroms.

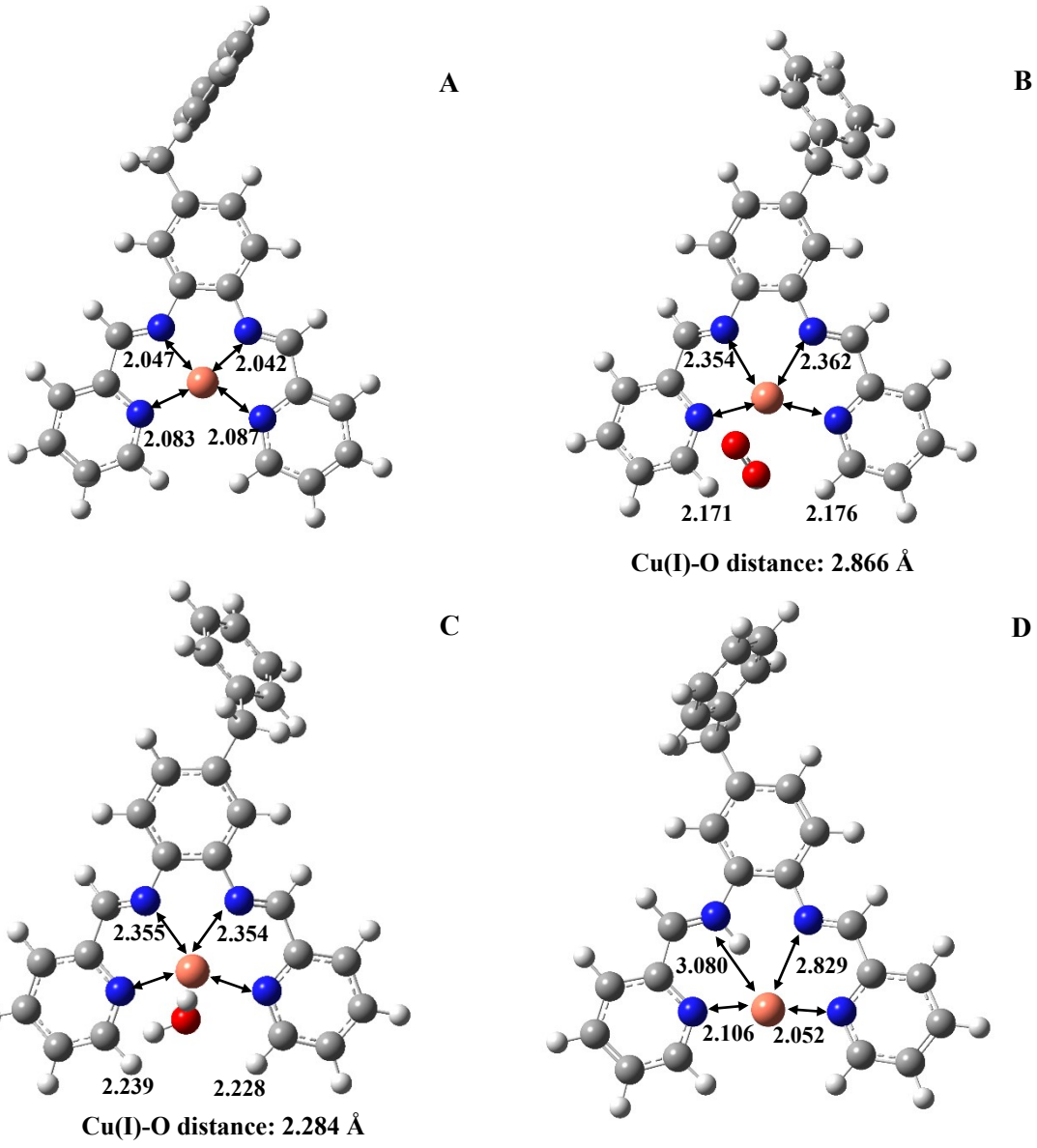

Figure S19. Optimized structures and distances between copper and nitrogen for: (A) complex 9-Cu(II);(B) reaction intermediate Cu(I)-O_2; (C) reaction intermediate Cu(I)-H_2O; (D) reaction intermediate Cu(I)-H^+. Distances are given in angstroms.

Table S22. Copper and oxygens distances given in angstroms for the nine complexes.

Complex	Cu(II) – superoxide distance	Cu(I) – dioxygen distance
1	2.5681	2.8807
2	2.3495	2.8630
3	2.0002	2.7010
4	2.3233	2.7653
5	2.3259	2.7190
6	2.2830	2.7631
7	2.3819	2.8852
8	2.2979	2.9691
9	2.3099	2.8549

Table S23. Copper and superoxide binding energies and BSSE corrections for the nine complexes.

Complex	Ligand EE(hartrees)	Superoxide EE(hartrees)	Ligand + Superoxide EE(hartrees)	BE (hartrees)	BSSE correction (hartrees)	BSSE Corrected BE kcal/mol
1	-2401	-150.32	-2551	-0.1457	0.0030	-91.42
2	-2440	-150.32	-2591	-0.1460	0.0032	-91.62
3	-2553	-150.32	-2704	-0.1228	0.0035	-77.06
4	-2632	-150.32	-2782	-0.1466	0.0030	-91.98
5	-2632	-150.32	-2782	-0.1465	0.0031	-91.94
6	-3473	-150.32	-3623	-0.1469	0.0030	-92.18
7	-2707	-150.32	-2857	-0.1452	0.0033	-91.13
8	-2863	-150.32	-3014	-0.1464	0.0032	-91.86
9	-2824	-150.32	-2974	-0.1469	0.0030	-92.20

Table S24. Copper and dioxygen binding energies and BSSE corrections for the nine complexes.

Complex	Ligand EE(hartrees)	Dioxygen EE(hartrees)	Ligand + Dioxygen EE(hartrees)	BE (hartrees)	BSSE correction (hartrees)	BSSE Corrected BE kcal/mol
1	-2401	-150.31	-2551	-0.0078	0.0019	-4.93
2	-2440	-150.31	-2591	-0.0069	0.0018	-4.32
3	-2554	-150.31	-2704	-0.0080	0.0019	-5.00
4	-2632	-150.31	-2782	-0.0078	0.0019	-4.90
5	-2632	-150.31	-2782	-0.0078	0.0019	-4.89
6	-3473	-150.31	-3623	-0.0078	0.0018	-4.87

7	-2707	-150.31	-2857	-0.0081	0.0020	-5.06
8	-2863	-150.31	-3013	-0.0081	0.0020	-5.07
9	-2824	-150.31	-2974	-0.0083	0.0019	-5.18